# The internal energy of CO 2 produced from catalytic oxidation of CO by NO

Daniel J. Bald and Steven L. Bernasek

Citation: The Journal of Chemical Physics **109**, 746 (1998); doi: 10.1063/1.476613
View online: http://dx.doi.org/10.1063/1.476613
View Table of Contents: http://scitation.aip.org/content/aip/journal/jcp/109/2?ver=pdfcov
Published by the AIP Publishing

# The internal energy of $CO_2$ produced from catalytic oxidation of CO by NO

Daniel J. Bald and Steven L. Bernasek
*Department of Chemistry, Princeton University, Princeton, New Jersey 08544*

(Received 23 February 1998; accepted 1 April 1998)

Internal energy distributions for $CO_2$ produced in the catalytic oxidation of CO by NO on polycrystalline platinum have been directly measured using a high-resolution tunable diode laser spectrometer. Absorption spectra have been collected for $CO_2$ produced in a flow cell reactor as a function of surface temperature and reactant ratio. Vibrational excitation of the product $CO_2$ is observed for all reaction conditions. The vibrational energy of the asymmetric stretching mode is higher than the bending and symmetric stretching modes. The level of vibrational excitation for all normal modes is sensitive to the NO:CO ratio. The observed internal energy distribution of the product $CO_2$ is compared to that of $CO_2$ produced from CO oxidation by $O_2$, using the same method. The similarities in the vibrational excitation and its dependence upon oxygen coverage suggest that the transition state for the $CO_2$ formation step is the same for both the CO+NO and $CO+O_2$ catalytic oxidation reactions. This similarity of likely transition states suggests that the CO+NO reaction proceeds by dissociative adsorption of NO, producing adsorbed oxygen atoms which oxidize CO to form $CO_2$. This is the same route to the formation of $CO_2$ which is observed for the $CO+O_2$ reaction on Pt. © *1998 American Institute of Physics.* [S0021-9606(98)70226-0]

## INTRODUCTION

The reaction between nitric oxide and carbon monoxide on platinum has practical importance in the removal of pollutants from combustion exhaust. The overall reaction is shown below in Eq. (1). Automobile emissions of nitrogen oxides ($NO_x$)

$$NO(g)+CO(g)\rightarrow \tfrac{1}{2}N_2(g)+CO_2(g) \tag{1}$$

are controlled by the after treatment of engine exhaust with catalytic converters that contain a mixture of three noble metals; Pt, Rh, and Pd. The removal of NO is also important from a kinetic point of view since the presence of NO is known to inhibit the catalytic oxidation of CO and hydrocarbons by oxygen.[1] All of these reactions are important in the removal of harmful components in automobile exhaust.

This reaction is also fundamentally important since it is slightly more complicated than the classical oxidation reaction of CO by oxygen. This system can provide the first test for the extension of any models developed, using the $CO+O_2$ reaction, to understand catalytic oxidation. The added complexity is due to both the production of molecules other than the oxidation product and the presence of additional surface species. These additional factors have the potential to either promote oxidation by opening up additional surface sites for reaction or inhibit oxidation by altering the surface energetics and relative surface concentrations by repulsive interactions.[2]

Unlike the catalytic oxidation of CO by $O_2$ on platinum which is insensitive to surface structure,[3] the CO+NO reaction is very sensitive to the surface structure of the metal. Studies using Pt(100) have shown high activity for reaction,[4–6] while Pt(111) has been shown to have very little activity.[7,8] The origin of this surface structure sensitivity is generally attributed to differences in NO dissociation rates.[8] Dissociation rates for NO have been shown to be dependent upon several factors; surface coverages of oxygen and CO,[8,9] availability of adjacent open surface sites, and coverage of NO.[10]

The reaction between CO and NO is considered to proceed by a Langmuir–Hinshelwood mechanism between two adsorbed species. However, there has not been complete agreement in the literature as to which of the surface species are involved in the $CO_2$ formation step. Most studies have suggested that NO dissociates to provide atomic oxygen which is scavenged by CO, similar to the $CO+O_2$ reaction.[11–14] However, several studies have proposed a bimolecular surface reaction between adsorbed NO and CO species to directly yield $CO_2$ as product.[9,15–17] The respective $CO_2$ formation steps for the two mechanisms are shown below.

Dissociative

$$CO(ad)+O(ad)\rightarrow CO_2(g). \tag{2}$$

Bimolecular

$$CO(ad)+NO(ad)\rightarrow CO_2(g)+N(ad). \tag{3}$$

The internal energy of $CO_2$ produced from CO oxidation by NO has not been probed previously. However, the dynamics of $CO_2$ produced from CO oxidation by $O_2$ has been investigated. The $CO_2$ product is found to desorb with excess translational[18–21] and vibrational[22–29] energy. For the system, changes in oxygen coverages have been found to affect the energy of the desorbing $CO_2$. In previous work,[22–24] the vibrational energy distribution of $CO_2$ produced from CO oxidation by $O_2$ was measured. An increase in vibrational energy for all modes was observed with increasing oxygen coverage. Ertl and co-workers[20,30] have seen sharpening of the desorption angular distribution with increasing oxygen coverage on Pt(111) surfaces. Mantell *et al.*,[26] using low-

 

resolution time resolved IR spectroscopy to track the vibrational spectrum of $CO_2$ produced from polycrystalline Pt foil, observed that the vibrational temperature increased with increasing oxygen coverage. In high-resolution IR emission studies for the reaction on Pd foil[28] an increase in the $O_2$:CO reactant ratio from 1:1 to 2:1 resulted in a significant increase in vibrational energy for all vibrational modes.

In the present study a tunable diode laser (TDL) is used to obtain the absorption spectrum of $CO_2$ produced in a flow cell reactor. Due to the high resolution of the TDL spectrometer ($0.001\ cm^{-1}$), single rotational transitions can easily be resolved and populations of individual states can accurately be determined. Flynn and co-workers[31–36] have demonstrated in collisional energy-transfer experiments that diode laser absorption spectroscopy is well suited for measuring vibrational energy distributions of $CO_2$. The relative population of any state can be determined, including the ground state (which cannot be probed with emission techniques) and ''IR inactive'' symmetric stretching states, by tuning the laser to a transition of the following type.

$$\nu_1 \nu_2^l \nu_3; J + h\nu(4.3\ \ \mu\mathrm{m}) \rightarrow \nu_1 \nu_2 l(\nu_3 + 1); J \pm 1, \qquad (4)$$

$\nu_1$ is the quantum number for the symmetric stretch mode, $\nu_2$ is the bending mode, $\nu_3$ is the asymmetric mode, and $J$ is the rotational quantum number. $l$ is the angular momentum associated with the doubly degenerate bending motion. Due to the large oscillator strength of the asymmetric stretch, all such transitions are allowed. The relative populations for states in each of the vibrational modes are used to determine individual Boltzmann temperatures which allows for energy deposition comparisons between the modes.

The $\nu_1, \nu_2, \nu_3, (r)$ notation used to denote a given vibrational band follows that of Rothman.[37] The symbol $r$ represents the level in the various Fermi-resonating groups. In this scheme all bands in a Fermi-resonating group have the same quantum numbers and the value of $r$ decreases with increasing band energy. The angular momentum associated with the bending motion is always equal to $\nu_2$ in this notation and will be omitted.

In the work reported here, high-resolution absorption spectroscopy is used to probe the internal energy of $CO_2$ produced by CO oxidation by NO on polycrystalline Pt in a flow reactor. To date almost all of the work in this area has used emission techniques to probe the vibrational and rotational energy of the desorbing $CO_2$. By using diode laser spectroscopy, the ground-state levels can be probed and a much higher resolution spectrum obtained. The vibrational energy distribution (and its dependence on reaction conditions) is compared to that observed for oxidation of CO by oxygen.[22] A significant increase in vibrational excitation as the NO/CO reactant ratio increases is also reported here. The similarity in vibrational excitation of the product $CO_2$ provides evidence that the same $CO_2$ formation step occurs for both oxidation reactions.

## EXPERIMENT

The flow reactor/diode laser spectrometer has been described in detail previously.[22] The flow cell is connected to a mass spectrometer chamber through a capillary placed in the center of the flow tube. A 60 l/s mechanical pump provides a linear flow of 1800 cm/s for a 1.7 Torr stream of high-purity argon. Electronic mass flow meters are used in each gas line to allow accurate measurement and control of reactant flow rates. The high-purity CO (Matheson 99.99%) and NO (Matheson 99.0%) were premixed behind a piezoelectric valve in order to insure consistent composition of the gases as they entered the established carrier gas flow. The platinum surface is a $3.5 \times 2.0$ cm piece of 100 mesh high-purity polycrystalline gauze.

The striped TDL is a standard Laser Photonics element tunable over the spectral region of the $CO_2$ asymmetric stretch, $2275-2340\ cm^{-1}$, in a series of modes ranging from 0.8 to $2.5\ cm^{-1}$ in width. The resolution of the spectrometer is better than $0.001\ cm^{-1}$. The infrared signal is detected by a 3 mm diameter 77 K InSb photovoltaic detector and preamplifier. The signal is amplified, then digitized and sent to a PC for data collection and manipulation. The same computer, through a Laser Photonics control module model L5820, controls the output of the laser during each sweep in a typical 1000 sweep data set. Frequency calibration was performed using a solid Ge etalon (free spectral range of $0.0482\ cm^{-1}$) as described previously.[22]

Prior to all reaction studies the platinum gauze was heated to 1100 K in a flow of 1.0 Torr of argon and 200 SCCM (standard cubic centimeters per minute) $O_2$ for 45 min in an effort to maintain consistent surface conditions. Checks of the steady-state reaction for a given gauze temperature and reactant ratio using the mass spectrometer showed constant levels of $CO_2$ production over a period greater than 5 h. This insured all data sets taken in a series probed the same density of product $CO_2$ molecules. Note that it was not imperative in these experiments to know absolutely how much $CO_2$ was being detected by the laser, it was only necessary to know that the effective pressure was constant.

The presence of contaminants in the NO reactant gas was taken into consideration during the absorption measurements. It was determined, initially from mass spectrometer measurements, that there was a significant amount of gas with a mass of 44 amu in the NO cylinder. This mass corresponds to $CO_2$ and $N_2O$, both of which are products of the CO+NO reaction under certain conditions and are unavoidable trace contaminants in the industrial purification of NO. The presence of both $CO_2$ and $N_2O$ were confirmed by their characteristic IR absorptions using the diode laser spectrometer. In order to avoid erroneous determination of relative rovibrational populations due to the absorption of $CO_2$ in the flow, the NO flow was maintained during the collection of the background spectrum. The background spectrum was taken in the absence of reaction (CO removed from flow) and subsequently divided by the spectrum taken during the reaction. This was done in order to account for fluctuations in the diode laser power with injection current. By using this procedure, no additional correction for the trace $CO_2$ needed to be performed.

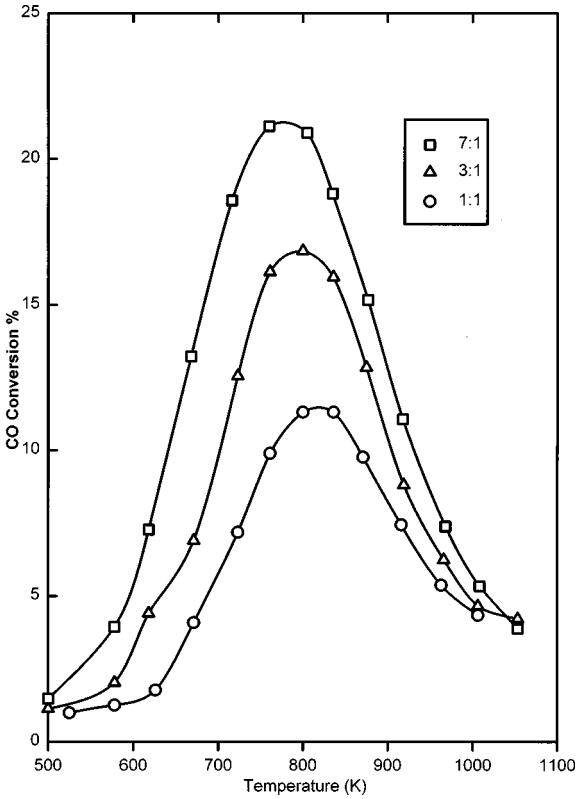


FIG. 1. CO conversion percentage as a function of surface temperature and reactant ratio. The three NO:CO reactant ratios (SCCM) are 7:1 (350:50), 3:1 (150:50), and 1:1 (50:50).

## RESULTS AND DISCUSSION

### Steady state kinetics

The production of $CO_2$ during the CO+NO reaction on polycrystalline Pt was followed as a function of temperature and reactant ratio using mass spectrometry and absorption spectroscopy. The results of the mass spectrometry study are compiled in Fig. 1 for three different NO:CO reactant ratios; 1:1, 3:1, and 7:1. The CO conversion percentage was obtained by simultaneously monitoring the CO and $CO_2$ signals and normalizing the CO:$CO_2$ ratio to the active cross section of the Pt gauze. A curve similar to Fig. 1 was obtained using the diode laser tuned to a single transition of the ground state (R18), monitoring the intensity as a function of temperature, and correcting for changes in rotational temperature.

The $CO_2$ production rate for the NO+CO reaction increases with increasing temperature beginning at 550–600 K. The reaction rate increases until a maximum is observed at a temperature, $T_{\max}$. The values of $T_{\max}$ are roughly 780, 800, and 820 for the 1:1, 3:1, and 7:1 reactant ratios, respectively. The actual reactant fluxes in standard cubic centimeters per minute (SCCM) for the three ratios were 50:50, 150:50, and 350:50. The total $CO_2$ production, and therefore CO conversion percentage, increases with increasing NO:CO ratio. The reaction rate decreases with increasing temperature above $T_{\max}$ until the reaction levels off at 1050 K. The $CO_2$ production rate determined from the IR absorption technique (which is more sensitive) goes to zero near 995 K.

The kinetics of the reaction vary substantially over the temperature range in Fig. 1. At the lower gauze temperatures, $T_G < T_{\max}$, the reaction is negative order in CO pressure and positive order in NO pressure. At $T_G > T_{\max}$ the reaction is seen to be positive order in CO pressure and slightly positive in NO pressure. The observed steady-state kinetics will be discussed in the context of the dissociation mechanism. This mechanism is the most widely accepted and allows for a straightforward interpretation of the observed results.

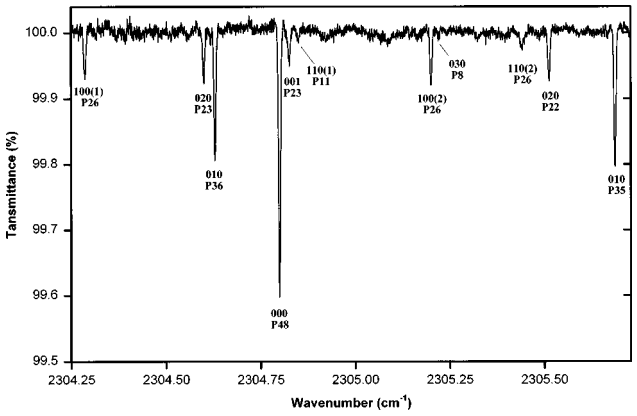


FIG. 2. A portion of the absorption spectrum collected for CO oxidation by NO at 800 K and a 5:1 NO:CO ratio.

At the lower temperatures, the observed kinetics are a result of the surface being covered predominantly by CO[3]. Adsorbed CO has been found to inhibit dissociation and adsorption of NO[8], so the reaction is initially limited by CO desorption. As the CO molecules desorb, sites are open for NO adsorption and dissociation into N(ad) and O(ad) species. Once an oxygen atom is on the surface it immediately combines with an adsorbed CO and is converted to the product. As the temperature is increased, more CO can desorb and the $CO_2$ production rate increases. In addition there is likely a significant amount of nitrogen atom recombination and desorption even at the lowest reaction temperatures. This will open up additional sites for NO adsorption and dissociation. Above $T_{\max}$, CO coverage on the surface has decreased and O coverage has increased, so that the reaction is limited by CO that adsorbs and reacts before desorbing. In addition, NO also may desorb from the surface before it is able to dissociate which would cause a decrease in the reaction rate.

## ABSORPTION MEASUREMENTS

Absorption spectra were collected for $CO_2$ produced from CO oxidation by NO on platinum under various reaction conditions. In some cases the surface temperature was changed while the reactant ratio remained constant and vice versa. A portion of a typical spectrum is shown in Fig. 2. This scan was taken at a 5:1 NO:CO ratio and 800 K surface temperature. It was obtained by sweep integration for 1000 iterations and subsequent division by the background laser intensity in the absence of CO in the flow. As mentioned above, there was a detectable amount of $CO_2$ as a trace gas in the NO source, so the background scan was taken with the NO flow maintained. Therefore any laser absorption from this $CO_2$ is divided out and does not affect the rovibrational population measurements. There is also a detectable amount

of $N_2O$ in the NO flow. $N_2O$ has been observed previously for CO oxidation by NO, but under the reaction conditions studied here, no product $N_2O$ was observed.

Normalized intensities from the absorption spectra were used to determine relative rovibration state populations. The procedure used to assign rotational and vibrational temperatures is identical to that used for the $CO+O_2$ reaction and is described in detail in Ref. 22. A rotational temperature for each vibrational band is calculated from the relative populations of different rotational states within a given vibrational state. The populations are fit to a Boltzmann distribution with the variable parameter being temperature. All of the bands exhibited the same rotational temperature for a given set of reaction conditions. This rotational equilibrium is due to the significant number of collisions with the Ar carrier gas as discussed previously.[22]

The vibrational Boltzmann temperatures for the $CO_2$ produced from the CO+NO reaction are determined by comparing the relative populations of vibrational bands, $Y_V$, to the vibrational energy of those bands. This population relative to $CO_2$ at 296 K is given by Eq. (5) below and is discussed in greater detail in Ref. 22.

$$Y_V = \ln \frac{I_N \nu_0}{S_{vj}^0} - \frac{BJ(J+1)}{k}\left(\frac{1}{T_0} - \frac{1}{T_J}\right) = \frac{E_V}{k}\left(\frac{1}{T_0} - \frac{1}{T_V}\right) + C. \quad (5)$$

In Eq. (5), $I_N$ is the normalized intensity, $S_{vj}^0$ is the line strength at 296 K from the HITRAN database,[38] $\nu_0$ is the line position, $E_V$ and $E_J$ are the vibrational and rotational energies, $T_0$ is 296 K, and $T_V$ and $T_J$ are the vibrational and rotational Boltzmann temperatures to be determined. $C$ represents terms which do not change during the course of the experiment. These include vibrational and rotational partition functions, path length, and molecular density. An average value of $Y_V$ is calculated for all rotational transitions detected within each band. This average value±one standard deviation is plotted versus $E_V$ for bands within a given vibrational mode and the best straight line through these points has a slope that is proportional to the vibrational Boltzmann temperature $T_V$.

The product $CO_2$ in these experiments undergoes a significant number of collisions with the three other gases in the flow (Ar, CO, and $O_2$). Most of the collisions occur with the Ar carrier gas. It was estimated that under experimental conditions (1.7 Torr) a $CO_2$ molecule has 1 100 Ar collisions during the time it takes to travel 2.5 mm downstream from the Pt gauze. The distance, 2.5 mm, conservatively estimates the average distance a molecule travels into the laser beam before it is detected. Using similar analysis it was estimated that product $CO_2$ would have 35–40 reactant gas collisions for a flux of 100 SCCM in the flow. The total number of collisions should ensure that the rotational state distributions are equilibrated. Based on collisional energy transfer rates,[39] each vibrational mode should also be well described by a Boltzmann distribution. However, the various modes should not necessarily be equilibrated with one another. The Fermi-resonant bending and symmetric stretching modes equilibrate relatively quickly with each other and any subsequent vibrational relaxation could affect both equally.[40] In order to mix with the Fermi-resonant modes, the asymmetric stretching mode requires nonresonant energy transfer which is a much slower process. In the data presented here the $\nu_1$ and $\nu_2$ modes are combined to one Fermi-resonant $\nu_1+\nu_2$ manifold, but the $\nu_3$ mode can be described by a distinct temperature.

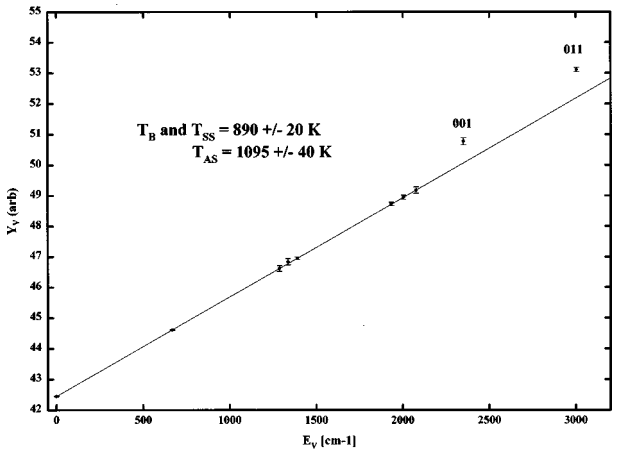


FIG. 3. A plot of relative vibrational population versus vibrational energy for all the $CO_2$ levels detected for a 10:1 NO:CO ratio. The straight line is drawn through all of the levels which correspond to the $v_1+v_2$ manifold, i.e., all except the 001 and 011 levels.

Figure 3 shows a plot of $Y_V$ versus $E_V$ for the CO+NO reaction at 800 K for a 10:1 NO:CO ratio. The straight line is drawn through all of the vibrational levels which correspond to either the bending or symmetric stretching mode. For this reaction system $Y_V$ for the bending and symmetric stretching modes are combined to obtain a single vibrational temperature. The temperature of the bending and symmetric stretching modes, $T_B$ and $T_S$, is determined from the relative populations of the 000, 010, 100(2), 020, 100(1), 110(2), 030, and 110(1) levels. The temperature of the asymmetric mode, $T_{\mathrm{AS}}$, is determined from the relative populations of both the 000 and 001 levels and the 010 and 011 levels.

Figure 4 shows the vibrational temperature for the normal modes as a function of reactant ratio for the CO+NO reaction at 800 K. All of the vibrational temperatures increase with increasing NO:CO ratios. $T_{\mathrm{AS}}$ is consistently greater than $T_B$ and $T_S$, and all of the temperatures are above the surface temperature. The rotational temperatures calculated at each of the reactant ratios are 680 K for 2:1, 690 K for 5:1, and 705 K for 10:1. All of the rotational temperatures are below surface temperature. As in the case of the $CO+O_2$ reaction, there is significant rotational relaxation and equilibration, which is a result of the $CO_2$ collisions with the argon carrier gas.

The relative vibrational population of $CO_2$ was obtained for the CO+NO reaction at a reactant ratio of 5:1 for two different reaction temperatures, 900 and 800 K. A rise in vibrational energy is observed that is commensurate with the increase in reaction temperature. This dependence of vibrational energy on reaction temperature is similar to that observed for the $CO+O_2$ reaction.[22] However, a more complete

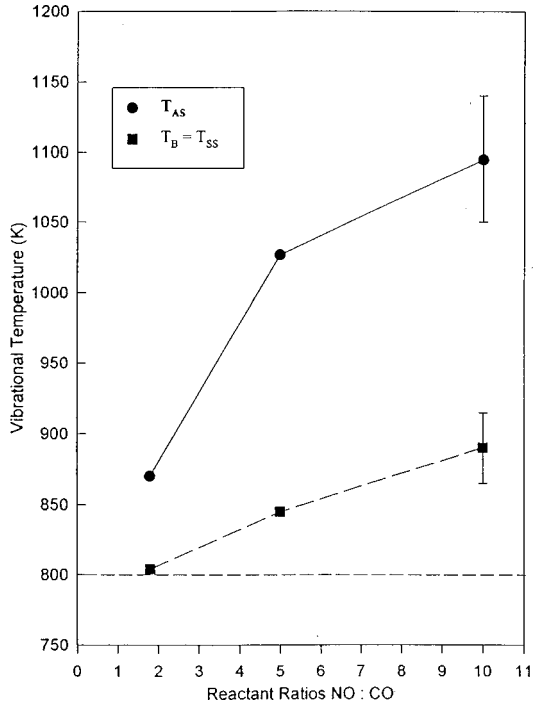


FIG. 4. Vibrational temperature of normal modes of $CO_2$ as a function of reactant ratio for the CO+NO reaction at 800 K.

survey of reaction temperatures is limited by signal levels. The $CO_2$ signal levels for the higher (and lower) temperature reaction were much lower because of the drop in reaction rate at 900 K (see Fig. 1).

The vibrational excitation of $CO_2$ produced from the NO+CO reaction is observed to increase with increasing NO:CO ratio. As in the case of the $CO+O_2$ reaction, an increased reactant ratio translates into higher coverages of that reactant. However, in the NO+CO reaction the correlation between reactant gas flux and surface coverage is more complicated than that for the $CO+O_2$ reaction. The complication arises from the additional process of NO dissociation (or nondissociation). In order to get an idea of the surface coverages during the reaction, two cases will be discussed; total dissociative adsorption of NO and no dissociation of adsorbed NO (bimolecular mechanism).

If all of the NO that adsorbs on the surface dissociates, one can correlate the reactant ratio to oxygen coverage in a manner similar to that discussed for the $CO/O_2$ system.[22,24] Several assumptions have to be made; (1) all of the NO that adsorbs immediately dissociates into atomic oxygen and nitrogen, (2) the sticking coefficient for NO is surface structure insensitive, (3) NO adsorption is first order with respect to vacant sites, (4) all of the atomic nitrogen immediately recombines and desorbs as $N_2$ thereby opening surface sites for additional NO adsorption, and (5) the CO surface coverage is relatively low. If all of these conditions are met, then the following equation can be used to estimate oxygen coverage on the Pt surface,[41]

$$\theta_O = \theta_{max}\{1 - X_{CO}/(S_O R)\}, \quad (6)$$

where $\theta_{max}$ (the maximum coverage of oxygen) corresponds to 0.5 ML,[42] $X_{CO}$ is the fractional CO conversion, $S_O$ is the sticking coefficient for nitric oxide which was taken to be 0.1 at 800 K,[8] and $R$ is the NO:CO ratio. The $\theta_O$ values obtained for the ratios in Fig. 1 are 0.12 at 2:1, 0.25 at 5:1, and 0.38 for 10:1. Assumptions 2–5 are all reasonable at the high temperature used for these measurements. Any deviation of these calculated coverages from the actual coverages will most likely be generated from a breakdown of the first assumption. As has been discussed earlier, NO dissociation does not readily occur under some reaction conditions and is inhibited by O(ad) and CO(ad). If the reaction proceeds by the bimolecular mechanism, altering the reaction ratio should vary the surface coverage of NO in a similar way. The maximum coverage of NO on the surface is 0.75 ML[10] so the only difference in the NO and O coverages determined from Eq. (6) would be a factor of 1.5.

The coverages determined from Eq. (6) are only rough estimates of the surface coverages for oxygen (or nitric oxide). At first approximation, the correlation between reactant ratio and oxygen coverage is half that for the $CO/O_2$ system. Essentially, there are two factors which dictate the relative oxygen coverage for a given set of reaction conditions, oxygen atom content of the oxidant gas and efficiency of CO conversion. A reaction with a 10:1 NO:CO ratio has the same oxygen coverage as a reaction with a 5:1 $O_2$:CO ratio at the same CO conversion percentage. However, the conversion percentage of the NO+CO reaction is generally smaller than that of the $CO+O_2$ reaction. This means the oxygen coverage for the former reaction is probably more than half of the oxygen coverage of the latter reaction at the same reactant ratios.

## COLLISIONAL DEACTIVATION

One of the factors that must be considered when interpreting the internal energies observed for $CO_2$ in the flow reactor experiment is collisional cooling by the other gases in the cell (Ar, NO, and CO). A complete discussion of the effect of $CO_2$–Ar and $CO_2$–CO collisions on the nascent internal energy distribution of carbon dioxide is provided in Ref. 22. Most of the $CO_2$ collisions that occur in the flow reactor are with Ar. These collisions cause complete rotational equilibration with the flow and vibrational equilibration within each normal mode, but little vibrational deactivation occurs. The $CO_2$–CO collisions are more efficient at vibrational deactivation of the $CO_2$, but literature values for deactivation rates[43,44] suggest any vibrational cooling would disproportionately affect the $\nu_3$ mode as opposed to the $\nu_1 + \nu_2$ manifold. An additional factor in the CO+NO reaction is the deactivation efficiency of $CO_2$–NO collisions.

In order to track energy leakage from the normal modes due to $CO_2$–NO interactions, one can consider the deactivation rates of the (010) level and (001) level of $CO_2$. In the case of $CO_2$ (001) deactivation by NO, the processes involved are shown in the following equations.

$$CO_2(001) + NO(0) \rightarrow CO_2(110) + NO(0) + 272\ cm^{-1}, \quad (7)$$

$$CO_2(001) + NO(0) \rightarrow CO_2(000) + NO(1) + 474\ cm^{-1}. \quad (8)$$

The $V$-$R,T$ process in Eq. (7) most likely dominates because of the lower $\Delta E$, but both processes contribute to the (001)

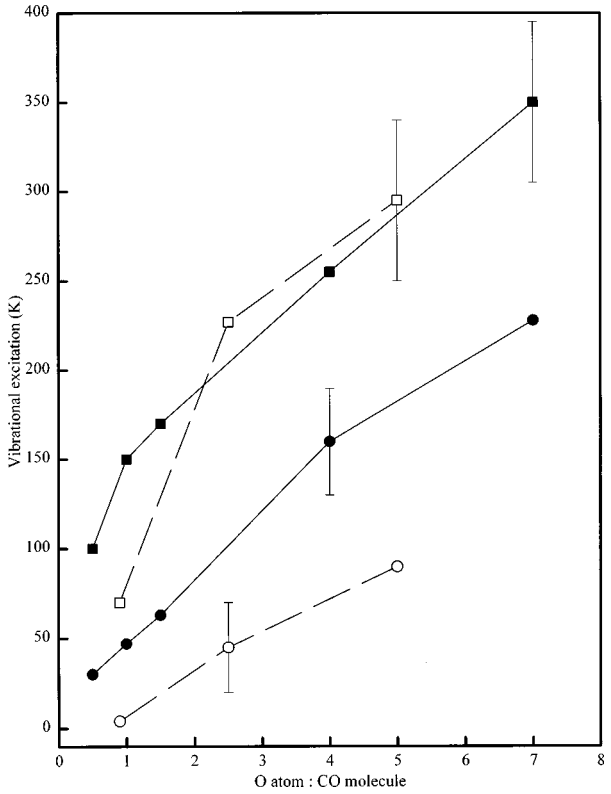


FIG. 5. A plot of vibrational excitation ($T_{\text{vibration}}$-$T_{\text{reaction}}$) versus O atom: CO ratio for both the CO+NO (open data points) and CO+$O_2$ (from Ref. 22, filled data points) reactions.

deactivation. The deactivation probability of the (001) state by NO is approximately $1\times10^{-4}$ at 700 K.[45] This is roughly five times greater than the deactivation probability in a $CO_2$–$O_2$ collision.[45]

The $CO_2$ (010) level relaxes to the ground state by the $V$-$R,T$ process shown in Eq. (9)

$$CO_2(010)+NO(0)\rightarrow CO_2(000)+NO(0)+667\ \text{cm}^{-1}. \quad (9)$$

Published results indicate[46] that the vibrational deactivation probability for process (9) is $7\times10^{-5}$. Collisional relaxation of $CO_2$ by NO should not be significant under the flow conditions of this study. We observe an increase in vibrational temperature for each of the modes as the amount of NO (and correspondingly $CO_2$–NO collisions) increases, as was the case for $CO_2$–$O_2$ collisions in the CO+$O_2$ reaction. Therefore any additional deactivation of the nascent $CO_2$ by NO is either negligible or small compared to the increased excitation.

### Comparison to CO+$O_2$ reaction

By comparing both the internal energies of the $CO_2$ produced from the CO+NO and CO+$O_2$ reactions, and the coverage dependence of those internal energies, we provide evidence which supports one of the proposed reaction mechanisms for CO oxidation by NO. Figure 5 shows the change in vibrational excitation for $CO_2$ produced from both of the reaction systems as a function of oxygen atom to CO molecule ratio. One should keep in mind that the reaction temperature is 800 K for the CO+NO reaction and 900 K for the CO+$O_2$ reaction. Therefore the vibrational excitation is described here as the difference between the surface temperature and the vibrational Boltzmann temperature. In addition, the vibrational temperatures of the $\nu_1$ and $\nu_2$ modes for the CO+$O_2$ reaction were combined to obtain a single vibrational temperature for these Fermi-resonant modes. Both the vibrational excitation and its dependence upon reactant ratios are similar for the two reaction systems. This provides strong evidence that the $CO_2$ formation steps for the two systems are the same, which suggests the NO+CO reaction proceeds by the dissociation mechanism.

The internal energy distribution of $CO_2$ produced in the catalytic oxidation of CO has been linked to the geometry and energetics of the surface transition state.[28] This was discussed in the context of the CO+$O_2$ reaction previously.[22] Although exact transition state geometries and energies are difficult to extract directly from the $CO_2$ internal energies measured under the conditions in this study, conclusions can be drawn from comparisons of different reactions. The $CO_2$ produced in the CO+NO reaction exhibits the same preferential channeling of energy into the asymmetric mode as was observed for $CO_2$ produced in the CO+$O_2$ reaction. Also, the vibrational energies are directly proportional to oxygen coverage in both systems, which indicates a similar coverage-dependent shift in potential energy of the transition state. Vibrational excitation of the $\nu_1+\nu_2$ manifold for the $CO_2$ produced from the CO+NO reaction is marginally lower than that for oxidation by $O_2$. This may indicate that the transition state has a slightly different geometry, possibly a larger O–C–O angle. The observed similarities in vibrational excitation trends suggest that the transition state for the $CO_2$ formation step is very similar for each of the reaction systems. Therefore the $CO_2$ formation step involves a reaction between adsorbed oxygen and CO [Eq. (2)] which is consistent with the dissociation mechanism for the CO+NO reaction.

However, there is a small difference in vibrational excitation of the Fermi-resonant modes of the product $CO_2$ as shown in Fig. 5. The $T_{SS}$ and $T_B$ are lower for the NO+CO reaction than for the CO+$O_2$ reaction for the same reactant ratio. This suggests that the transition state for the NO+CO reaction is less bent than the transition state for the CO+$O_2$ reaction. Alternatively, the difference in vibrational excitation of the Fermi-resonant modes could result from the different collisional deactivation properties of NO and $O_2$. It is difficult to draw any strong conclusions since the equilibration of the two normal modes clouds the issue somewhat.

In contrast, if the NO+CO reaction occurs by the bimolecular mechanism [Eq. (3)] one would expect to observe a drastically different internal energy distribution in the product $CO_2$. The transition state energetics for the $CO_2$ production step would most likely be less sensitive to adsorbate coverage and any similarities in vibrational excitation for the two oxidation reactions would be fortuitous. The transition state geometry, potential energy, and the energy available to the nascent $CO_2$ should all be different for the two reactions. Presumably, the transition state for reaction 3 would involve OC–O bond formation in conjunction with N–O bond cleavage. The transition state for the CO+$O_2$ reaction involves OC–O bond formation in conjunction with Pt–O bond cleav-

age. As has been discussed previously,[22] the origin of the vibrational excitation coverage dependence is likely a change in the Pt–O bond strength which alters the potential energy of the transition state. The N–O bond strength should be less affected by changes in surface coverage, or at least have a different coverage dependence. Also, in the bimolecular reaction the $CO_2$ would desorb from association with a nitrogen atom on a Pt surface, while in the dissociative reaction the nascent $CO_2$ desorbs directly from the Pt surface. This would be expected to drastically alter any energy transfer between desorbing $CO_2$ and the surface, and thus the observed $CO_2$ internal energy would be expected to be different.

## CONCLUSION

Internal energy distributions for $CO_2$ produced in the CO+NO reaction on platinum have been directly measured using a high-resolution tunable diode laser spectrometer. Vibrational excitation of the product $CO_2$ is observed for all reaction conditions. The vibrational energy of the asymmetric stretching mode is greater than the vibrational energy of the bending and symmetric stretching modes over all reaction conditions. The level of vibrational excitation for all normal modes is sensitive to surface oxygen coverage. The observed internal energy distributions of the product $CO_2$ are compared to the distributions measured for $CO_2$ produced from CO oxidation by $O_2$. The similarities in the vibrational excitation and the dependence of vibrational excitation upon oxygen coverage suggest that the transition state for the $CO_2$ formation step is very similar for both the CO+NO and $CO+O_2$ reactions. This correlation provides evidence that the CO+NO reaction proceeds by a mechanism wherein the NO dissociates to produce adsorbed oxygen atoms, and not a bimolecular mechanism between adsorbed NO and CO. The slightly lower vibrational excitation of the Fermi-resonant modes of the product $CO_2$ when the NO+CO reaction is compared with the $O_2$+CO reaction suggests that the transition state for $CO_2$ production in the NO+CO reaction may be less bent. Detailed modeling would be needed to more fully characterize the transition state in these reactions.

## ACKNOWLEDGMENT

This research was supported by the Chemistry Division of the National Science Foundation.

[1] K. C. Taylor, Catal. Sci. Technol. **2**, 133 (1984).
[2] V. P. Zhdanov, Surf. Sci. **165**, L31 (1986).
[3] T. Engel and G. Ertl, Adv. Catal. **28**, 1 (1979).
[4] M. W. Lesley and L. D. Schmidt, Surf. Sci. **155**, 215 (1985).
[5] S. B. Schwartz and L. D. Schmidt, Surf. Sci. **183**, L269 (1987).
[6] M. W. Lesley and L. D. Schmidt, Chem. Phys. Lett. **102**, 459 (1983).
[7] R. E. Hendershot and R. S. Hansen, J. Catal. **98**, 150 (1986).
[8] R. J. Gorte and L. D. Schmidt, Surf. Sci. **111**, 260 (1981).
[9] E. W. Scharpf and J. B. Benziger, J. Catal. **136**, 342 (1992).
[10] M. J. Mummey and L. D. Schmidt, Surf. Sci. **109**, 43 (1981).
[11] D. Lorimer and A. T. Bell, J. Catal. **59**, 223 (1979).
[12] R. M. Lambert and C. M. Comrie, Surf. Sci. **46**, 61 (1974).
[13] Y. O. Park, W. F. Banholzer, and R. I. Masel, Surf. Sci. **155**, 341 (1985).
[14] T. Fink, J. P. Dath, M. R. Basset, R. Imbihl, and G. Ertl, Vacuum **41**, 310 (1990).
[15] H. Miki, T. Nagase, T. Kioka, S. Sugai, and K. Kawasaki, Surf. Sci. **225**, 1 (1990).
[16] R. L. Klein, S. Schwartz, and L. D. Schmidt, J. Phys. Chem. **89**, 4908 (1985).
[17] B. A. Bance, D. T. Wickman, and B. E. Koel, J. Catal. **119**, 238 (1989).
[18] R. L. Palmer and J. N. Smith, Jr., J. Chem. Phys. **60**, 1453 (1974).
[19] C. A. Becker, J. P. Cowin, L. Wharton, and D. J. Auerbach, J. Chem. Phys. **67**, 3394 (1977).
[20] J. Segner, C. T. Campbell, G. Doyen, and G. Ertl, Surf. Sci. **138**, 505 (1984).
[21] E. Poehlmann, M. Schmitt, H. Hoinkes, and H. Wilsch, Surf. Sci. **288**, 26 (1993).
[22] D. J. Bald, R. Kunkel, and S. L. Bernasek, J. Chem. Phys. **104**, 7719 (1996).
[23] S. L. Bernasek and S. R. Leone, Chem. Phys. Lett. **84**, 401 (1981).
[24] L. S. Brown and S. L. Bernasek, J. Chem. Phys. **82**, 2110 (1985).
[25] D. A. Mantell, S. B. Ryali, B. L. Halpern, G. L. Haller, and J. B. Fenn, Chem. Phys. Lett. **81**, 185 (1981).
[26] D. A. Mantell, S. B. Ryali, and G. L. Haller, Chem. Phys. Lett. **102**, 37 (1983).
[27] M. Kori and B. Halpern, Chem. Phys. Lett. **98**, 32 (1983).
[28] G. W. Coulston and G. L. Haller, J. Chem. Phys. **95**, 6932 (1991).
[29] H. Uetsuka, K. Watanabe, and K. Kunimori, Surf. Sci. **363**, 73 (1996).
[30] C. T. Campbell, G. Ertl, H. Kuipers, and J. Segner, J. Chem. Phys. **73**, 5862 (1980).
[31] J. O. Chu, G. W. Flynn, and R. E. Weston, Jr., J. Chem. Phys. **78**, 2990 (1983).
[32] J. O. Chu, C. F. Wood, G. W. Flynn, and R. E. Weston, Jr., J. Chem. Phys. **80**, 1703 (1984).
[33] J. O. Chu, C. F. Wood, G. W. Flynn, and R. E. Weston, Jr., J. Chem. Phys. **81**, 5533 (1984).
[34] J. A. O'Neill, C. X. Wang, J. Y. Cai, G. W. Flynn, and R. E. Weston, Jr., J. Chem. Phys. **88**, 6240 (1990).
[35] J. A. O'Neill, T. G. Kreutz, and G. W. Flynn, J. Chem. Phys. **87**, 4596 (1987).
[36] T. G. Kreutz, J. A. O'Neill, and G. W. Flynn, J. Phys. Chem. **91**, 5540 (1987).
[37] L. S. Rothman, Appl. Opt. **25**, 1795 (1986).
[38] L. S. Rothman, R. R. Bamache, A. Goldman, L. R. Brown, R. A. Toth, H. M. Pickett, R. L. Poynter, J.-M. Flaud, C. Camy-Peyret, A. Barbe, N. Husson, C. P. Rinsland, and M. A. H. Smith, Appl. Opt. **26**, 4058 (1987).
[39] J. Finzi and C. B. Moore, J. Chem. Phys. **63**, 2285 (1975).
[40] F. Lepoutre, G. Louis, and H. Manceau, Chem. Phys. Lett. **48**, 509 (1977).
[41] G. W. Coulston and G. L. Haller, in *Surface Science of Catalysis*, edited by D. J. Dwyer and F. M. Hoffman (ACS, Washington, DC, 1992), Vol. 58, p. 482.
[42] J. L. Gland, B. Sexton, and G. Fisher, Surf. Sci. **95**, 587 (1980).
[43] J. C. Stephenson, R. E. Wood, and C. B. Moore, J. Chem. Phys. **54**, 3097 (1971).
[44] J. C. Stephenson and C. B. Moore, J. Chem. Phys. **56**, 1295 (1972).
[45] S. H. Bauer, J. F. Caballero, R. Curtis, and J. R. Wiesenfeld, J. Phys. Chem. **91**, 1778 (1987).
[46] C. B. Moore, in *Fluorescence: Theory, Instrumentation, and Practice*, edited by G. G. Giuilbault (Marcel Dekker, New York, 1967).